Characterization and Improvement of 800ns Implosion Time Aluminum Nested Arrays on Sphinx Machine [1]

H.Calamy, F.Lassalle, F.Bayol, C.Mangeant, F.Hamann, A.Morell, J.P.Bedoch, P.Combes, S.Ritter, J.Chittenden*, S.Lebedev**

Centre d'Etudes de Gramat, 46500 Gramat, France
* Imperial College, London

Abstract − The SPHINX machine based on microsecond LTD technology is used in direct drive mode to implode nested aluminum wire arrays with outer diameter up to 140mm and maximum current from 3.5MA to 4.5MA. Experimental setup and diagnostics are described. Characterization includes implosion dynamics, study of ablation phase and the radial and axial radiations measurements. 2D simulations are presented. The behavior of z-pinches wire arrays in this 800ns regime appears very similar to those observed on shorter implosion time (60ns to 300ns) machines and the main results are changed in a self-consistent manner with the current rise time. Influence of current return can geometry upon the homogeneity of implosion and interaction of nested arrays are analyzed. SPHINX results show radial radiations with 1-3TW total power, 100-300 kJ total energy and 20kJ-30kJ energy above 1keV; axial total power reaches around 0.1TW.

1. Introduction

Sphinx generator (5 MA, 1μs rise time [1]) is used for studies of Z-pinch K-shell radiation sources. The load is an aluminum nested wire array with outer array radius of 7 cm, inner array radius 3.5 cm, height 5 cm, wire diameter 10.4 μm, number of outer array wires between 198 and 120, and number of inner array wires between 99 and 50. Diagnostic package description can be found in [2].

This paper presents typical results of Sphinx shots and points out some physical features observed. Current distribution is studied, effect of the return current conductor geometry is shown. Axial inhomogeneity of the implosion is highlighted and first results of pre-pulse current studies are given.

2. Experimental results

The first goal of Sphinx machine was to obtain a reliable X-ray source for radiation effects studies. Therefore efforts have been put on maximizing the K-shell yield of aluminum wire arrays. Sphinx loads were first single wire arrays that gave very unstable implosion

with a dramatic lack of reproducibility and poor k-shell yield of about 1-2 kJ. The benefit of using nested array configurations was then proved for the stabilization and reproducibility of the source. Simultaneous improvements of the generator leading to a charging voltage of the capacitors of 60kJ were made [1]. A typical result of Sphinx shots with 780 ns implosion time is shown on Fig. 1.
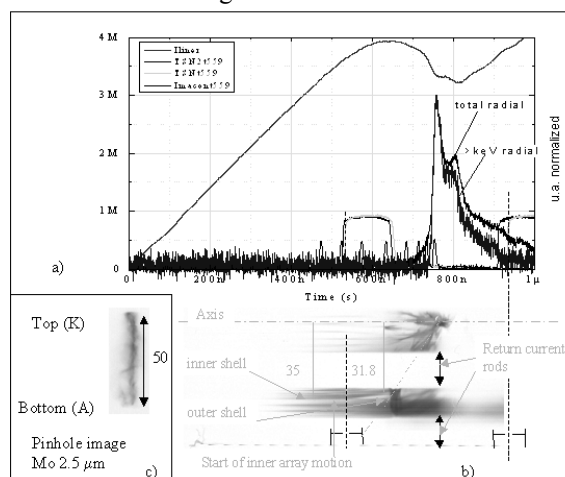
Fig. 1 : Typical result. Shot 559-50kV :a) current in the load, normalized total and k-shell power. b) streak camera image; axis and initial dimension of the inner array are shown. The image is put in order to have the same time base as fig 2a). The motion of inner array before arrival of the outer array implosion is highlighted. c) time-integrated pinhole image

Similar phenomena as those observed on faster wire array implosion are observed on Sphinx. The implosion can be cutted in four different phases as described in [3]. After the first initiation phase, wires remain at their initial position for ~500 ns. During this period named ablation phase, the wire forms a core-corona structure [4].Current is flowing in the conducting corona and precursor plasma is injected towards the axis before the start of the main implosion. One of the specific features of long implosion time wire array is that a fraction of the current (~30 %) can flow in the inner array 400 ns before the start of the main implo-

sion of the outer array. The start of the implosion corresponds to an increase of the pinch voltage (see [2]) as the outer array wires runs out of material generating a sudden increase of dI/dt. This time is named the ablation. Fig. 2 shows the ablation time measured for nested arrays with varying number of inner array wires while all other parameters are left unchanged. It is seen that the ablation time is affected by the inner array design, increasing as the number of inner array wires increases and that the presence of an inner array increases the ablation time of at least 40 ns compared to a single array. To match the experimental ablation time of the outer array with the rocket model [4] we need to make the assumption that only a fraction of the total current i.e. 70% flows in the outer array (ablation velocity is 15 cm/μs). On streak camera images (see Fig. 1), the inner array is seen to have an initial motion before the arrival of the imploding outer array. This phenomenon can be explained by the remaining part of the current flowing into the inner array wires. The reason of this current repartition might be the resistive contribution to the current division between the arrays should not be neglected in our nested wire arrays. In this case the current in the inner array can be found from the following differential equation [5]:

$$R_{out}I_{out}+L_{out}\frac{dI_{out}}{dt}+M\frac{dI_{in}}{dt}=R_{in}I_{in}+L_{in}\frac{dI_{in}}{dt}+M\frac{dI_{out}}{dt} \quad (2)$$
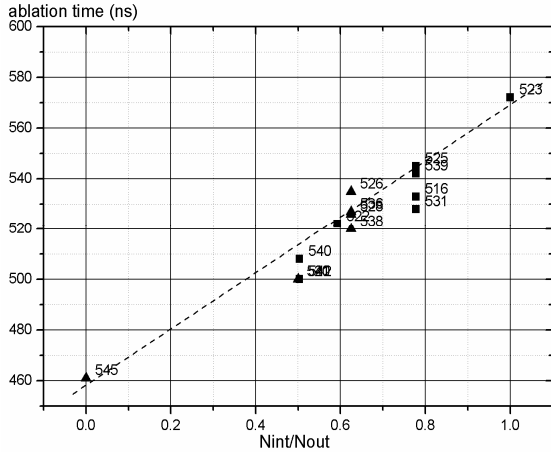

Fig. 2: Ablation time deduced from electrical measurements versus ratio of inner to outer array wires. Labels are shot numbers. All shots except 545 were nested array with outer array radius of 7 cm, inner array radius 3.5 cm and height 5 cm. Shot 545 is a single array corresponding to a single outer array (radius of 7 cm, height 5 cm). Number of wires for outer array is 144 (triangles) or 135 (squares)

The data can therefore be organised taken into account resistive division. Fig. 3 shows that configuration leading to a reduced initial displacement of the inner array does correspond to shots giving the best K-shell yield. That is to say that the effect of the resistive

term can be detrimental to the implosion stability probably because of less R-T mitigation as both arrays collide at smaller radius.
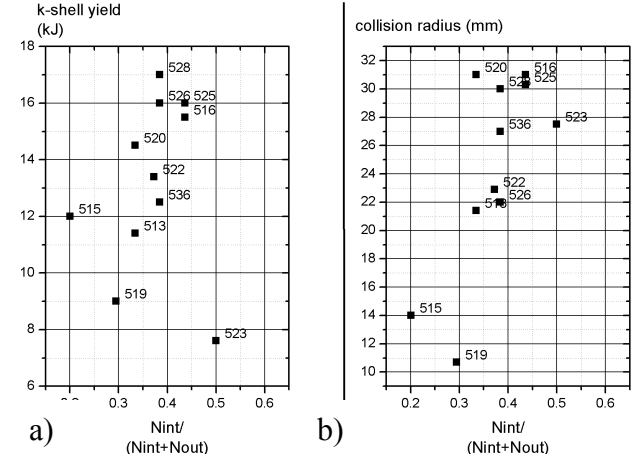

Fig. 3: a) K-shell yield versus resistive division. A relative optimum is obtained around value of 0.4 with a dramatic decrease when going to 0.5. Numbers are shot labels b) Collision radius of outer and inner array versus resistive division. The smallest displacements are obtained for value from 0.35 to 0.45

3. Influence of current return can geometry

The return current conductor (RCC) used on Sphinx shots has usually sixteen diagnostic apertures of 20 mm width and the RCC-outer array gap is 1 cm wide. This geometry is found to have a strong effect on the magnetic field topology and also on the magnetic pressure on the outer array wires. Numerical simulations show that this geometry gives an initial modulation of the magnetic field of about 14 % on the outer array wires.

MHD simulations with 2Drθ Gorgon code (Fig.4) show that the wires that are close to the metal wall of the RCC have slightly higher current than those close to the aperture and ablate slightly faster. This azimuthal inhomogeneity makes that both the precursor flow and the implosion are now focussed not on the axis but on a point just outside the inner array. One imploding clump per RCC is therefore formed during the implosion. This effect is experimentally observed on visible streak camera images. After the strike of the outer array onto the inner one, these sixteen clumps are really bright because they carry the majority of the current. It creates filaments that can be seen on the streak camera images (Fig.4). However, this azimuthally perturbated implosion does not seem to have to much detrimental effect on both total power and k-shell yield. Shots have been done to reduce this effect. Increasing the number of RCC apertures to reduce the azimuthal inhomogeneity of the magnetic field to less than 1%, installing wires with an irregular inter-wire gap to restore best homogeneity of the main implosion

shell just before the strike with the inner array were tests that have been done. No more filaments were seen on streak images as expected but neither an increase of the K-shell yield nor of the total power was obtained.
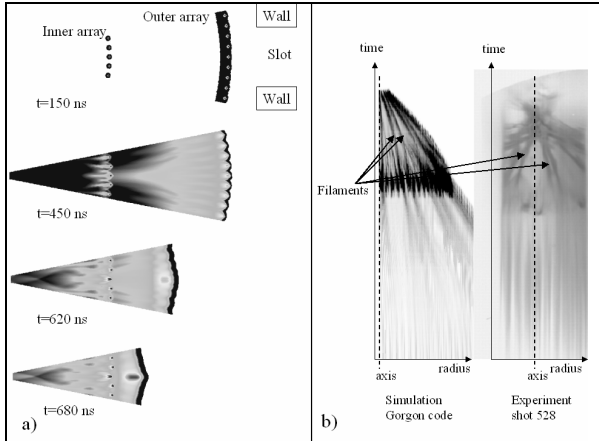

Fig.4: Results of 2Dr-θ MHD simulations (Gorgon). Density profiles at 150,450,620 and 680ns just before collision of the two arrays b) reconstructed streak camera image. The radiated power calculated by the code is taken as a representative output for the light emitted; the signal on the camera is then deduced thanks to geometric calculations. On the right is shown the experimental image from the camera for shot 528
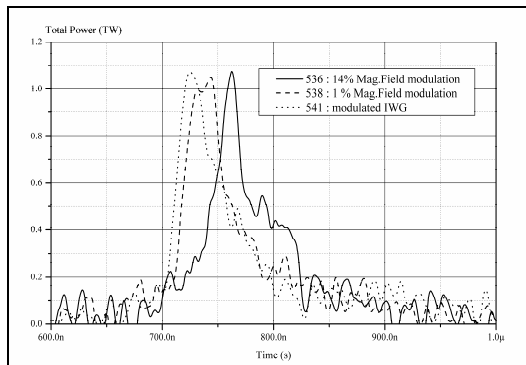

Fig.5: Evolution of radiation pulses power of shots 536,538,541. Load design varies to go from 14% initial magnetic field modulation (solid) to 1% (dashed). Irregular inter wire gap is used for shot 541(dotted)

4. Axially modulated ablation rate

Zippering of the pinch is observed on almost every shot. The effect can be seen on optical images (seeFig.6) or on zipper array data[2]. The mass near the cathode seems to implode earlier and radiate first as the rest of the mass is still in the process of the implosion. On the contrary the framing camera images also show that the formation of the precursor plasma column starts at the anode and his height increases in

time from anode to cathode. This observation that we called on other paper [7] as the "plasma bridge" problem, can be explained by an axial modulation of the ablation velocity. Assuming that this parameter is lower near the cathode than near the anode and increases from cathode to anode, the result is that a smaller ablation rate is obtained near the anode. Thus the outer array wires run out of material first near the cathode and the implosion starts here. The start of the implosion is delayed near the anode because of a lower ablation rate. On the contrary, the precursor plasma flows towards the axis with a bigger velocity and a smaller density near the anode leading to the formation of the precursor plasma column near the anode first. The origin of this modulation of the ablation rate is not yet well understood. A good candidate could be the effect of the radial electric field. It was shown in [8] that the ablation phase of wire array can be strongly affected by the radial electric field. On Sphinx load geometry, the radial electric field is negative near the cathode and becomes lower and lower going to the anode. Further studies are on going to study and understand this effect. It is important to note here that two shots (#507-#508) were done on positive polarity. For these shots, a delayed implosion was observed: radiation pulse occurs ~100 ns later than for the same load configuration in negative polarity. It might confirm that the ablation regime is strongly affected by the radial electric field. The fact that this phenomenon was observed on Sphinx and on faster generator (Magpie [8]) implies that it is not a specific feature of long implosion time wire arrays.
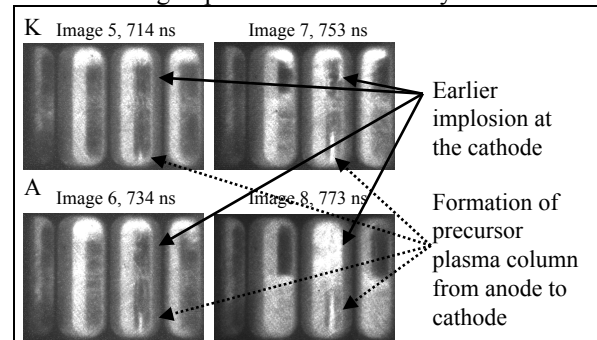

Fig.6 : framing camera images of shot 543 showing axially inhomogeneous implosion

5. Effect of a current prepulse

Sphinx generator configuration allows to inject a long current prepulse on the wire array load before the start of the main current [1]. The maximum of this current prepulse was ~10 kA with a 50 μs rise time. Rough calculations show that the energy deposited in the wires during the prepulse is enough to reach the melting. Similar studies had been made in the past on the effect of a current prepulse[6]. This prepulse dramatically changes the implosion and the load behaviour.

First a brighter precursor plasma pinch is observed on optical diagnostics. This precursor forms at around ~400 ns indicating an average velocity of about 20 cm/µs. The precursor then expand and is hitted by the arrival of the main implosion. No more motion of the inner array is observed which might indicate that the modification of the initial state of the outer array wires prevent the current to flow in the inner array. The implosion is delayed and the radiation pulse occurs ~100 ns later than for similar shots without current prepulse.
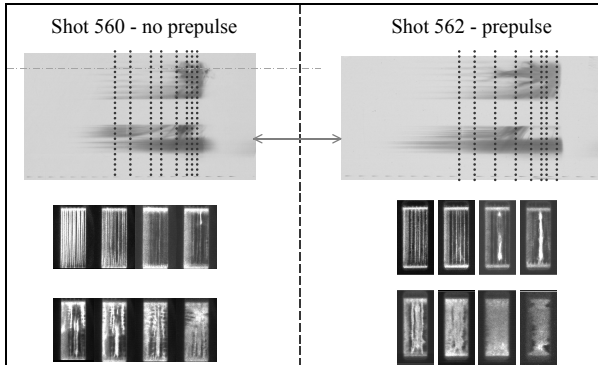

Fig. 7 : Modification of implosion characteristics due to prepulse. Streak camera and framing camera images. The dotted lines corresponds to frame time

The most important result obtained is that the radiation pulse is strongly improved. The full width at half maximum (FWHM) goes from 40-50 ns to 20 ns with a reproducible behaviour (

Fig. 8). The total radiated energy increased from 100 kJ to 160 kJ. The total power is multiplied by a factor of 4. The last shot of this series gave the best K-shell yield ever obtained on Sphinx : 6.3 kJ/cm with a FWHM of 23 ns. Further experiments will be done to confirm these first results.
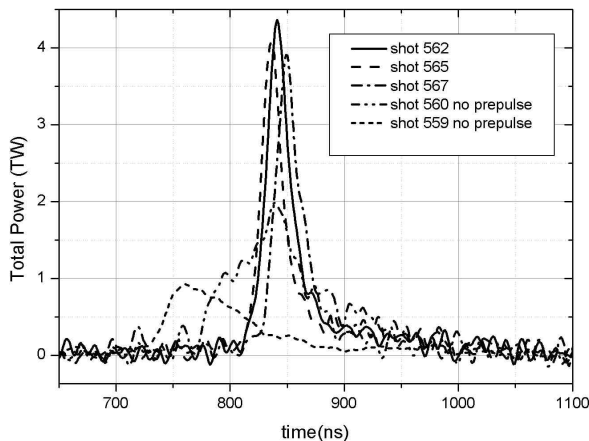

Fig. 8 : Variation of x-ray pulse with and without current prepulse

Again the question of how the current prepulse affects the implosion dynamics raises the question of ablation regime of the outer array wires. Delayed implosion and formation of a more bright precursor plasma column can be explained by an increased ablation velocity. As it was seen that relation between ablation velocity and radial electric field is strong, a good candidate could be to explain prepulse current effect is that it can alter the radial electric field

6. Conclusion

Z pinches experiments done on Sphinx generator show that good K-shell yield and total power can be achieved even with a slower rise time of the current. Similar physical features as faster z-pinch such as wire ablation, RCC geometry effect, radial electric field effect are observed showing that the same physical processes are activated and that slower rise time experiment might be a way to highlight key points of z-pinch physics. First results of long prepulse current shots are very encouraging and will be persued in the future.

7. Acknowledgment

8. References

[1] F.Lassalle et al., "Reliability and Performances Improvements of the SPHINX Machine Based on the 1 Microsecond LTD Technology" presented at *14th Symp. on High Current Electronics*, Tomsk, Sept. 2006.

[2] H.Calamy et al., "SPHINX Machine diagnostic package for characterization of 800ns implosion time aluminum nested arrays" presented at *14th Symp. on High Current Electronics,* Tomsk, Sept. 2006.

[3] M.E. Cuneo et al, Phys. Rev.E, **71**, 046406 (2005) S.V. Lebedev et al., Phys. Rev. Lett, **81**, 4152, (1998)

[4] S.V.Lebedev et al., Physics of Plasma, **8**, 8, 3734, (2001)

[5] S.N.Bland et al, Physics of Plasmas, **10,** 4, 1100, (2003)

[6] F.Beg et al, Physics of Plasmas, **9**, 1, (2002)

[7] H.Calamy et al, *in AIP Conf. Proc.,* vol. 808, pp. 15-20, 2006

[8] S.V.Lebedev et al., Phys. Rev. Lett, **95**, 135001, (2005)